The Instability of a Viscoelastic Conducting Cylindrical Interface Supporting Free-surface Currents

Yusry O. El-Dib and Galal M. Moatimid

Department of Mathematics, Faculty of Education, Ain Shams University, Heliopolis, Cairo, Egypt

Reprint requests to Dr. G. M. M.; E-mail: gal_moa@hotmail.com

Z. Naturforsch. **57 a,** 159–176 (2002); received October 19, 2001

The stability of a viscoelastic interface acted upon by an oscillating azimuthal magnetic field is studied. The interface separates two rigid magnetic fluid columns. Only azimuthal disturbrance modes are considered in a linear perturbation technique. Weak viscoelastic effects are taken into consideration, so that their contributions are demonstrated in the boundary conditions. The presence or absence of free surface currents resulted in a dispersion equation with complex coefficients of the Mathieu type. It is found that the surface currents disappear when the stratified magnetic field becomes unity. The phenomenon of coupled resonance is observed. Several special cases are reported. A set of graphs are drawn to illustrate the influence of the various parameters on the stability of the considered system.

Key words: Hydrodynamic Interfacial Instability; Viscoelastic Fluids; Magnetic Fluids; Free-surface Currents.

1. Introduction

The interaction of electromagetic fields and fluids has attracted increasing attention with the promise of applications as diverse as controlled nuclear fusion, chemical reactor engineering, medicine, and high-speed silent printing. Viscoelastic fluids find applications in petroleum drilling, manufacturing of foods and paper, etc. As to hydromagnetic flow and heat-transfer, many metallurgical processes involve cooling of continuous strips of filament by drawing them through a quiescent fluid, and, during this process, these strips or filaments are sometimes stretched. Drawing, annealing, and tinning of copper wires produce similar effects. In all of these cases, the properties of the final product depend to a great extent on the rate of cooling. By drawing such strips or filaments in an electrically conducting fluid, subject to a magnetic field, the rate of cooling can be controlled and a final product, with desired characteristics, can be achieved. Another interesting application of hydromagnetics to metallurgy lies in the purification of molten metals from nonmetallic inclusions by the application of a magnetic field. The stability analysis of viscoelastic fluids has been attracted the attention of many authers [1 - 6]. In [1], two uniform fluids are separated by a horizontal boundary and the case of exponentially varying density has been considered for both viscous and viscoelastic fluids. It was found that the effective interfacial tension succeds in stabilizing perturbations of certain wave numbers (small wavelength perturbations) which were unstable in the absence of effective interfacial tension, for unstable configuration / stratification. The effect of a variable horizontal magnetic field and a uniform rotation was considered by Kumar [2]. He found that the presence of a magnetic field stabilizes a certain wave-number band, whereas the system is unstable for all wave-numbers in the absence of the magnetic field for the potentially unstable configuration. However, the system is stable in the potentially stable case and unstable in the potentially unstable case for highly viscous fluids in the presence of a uniform rotation. In [3], it was found that the stability criterion is independent of the effects of viscosity and visco-elasticity and is dependent on the orientation and magnitude of the magnetic field. It was also found that the magnetic field stabilizes a certain wave-number range of the unstable configuation. Sharma and Kumar [4] pointed out that the presence of a magnetic field introduces oscillatory modes which were non-existent in its absence. They also obtained the sufficient condition for the non-existence of overstability. In [5], it was found that for exponentially varying stratifications, the system becomes stable or

0932–0784 / 02 / 0300–0159 $ 06.00

unstable for stable and unstable stratifications under certain physical conditions, and the growth rates were found to increase or decrease with increasing stratification parameters, according to some restrictions satisfied by the chosen wavenumbers range. Recently, El-Dib [6] carried out the stability analysis of a viscous interface supporting free-surface currents in a hydromagnetic rotating fluid column. His analysis resulted in a nonlinear relation between the surface current density and both the stratified viscosity and the stratified azimuthal magnetic field. He also found that the angular velocity plays a destabilizing role, while the magnetic field frequency plays a stabilizing role and acts against the angular velocity effect.

The effect of a uniform rotation about the vertical axis on the development of the Kelvin-Helmholtz instability has been treated by Chandrasekhar [7]. He found that the rotation does not stablize the motion for any difference in the velocities in the absence of surface tension. The effect of surface tension on this rotating system has been investigated by Alterman [8]. He showed that in a rotating system, the surface tension fails to stabilize the motion for any difference of velocities and any angular velocity of the motion. For excellent reviews see Drazin and Reid [9]. Chung and Wuest [10] have shown that the rotation of liquid columns helps to stabilize the formation of a crystal. Destabilization effects are also important, particulary in the areas of chemical engineering and combustion: the break-up of liquid jets is enhanced by rotation, a process now referred to as swirl atomization. Rigidly rotating liquid columns are also known to support interesting linear [11] and nonlinear [12] free surface and internal waves. Wilson [13] investigated the effect of an axial magnetic field on the capillary instability of an infinitely long cylindrical fluid column. He obtained a general analytical solution to the linearized problem and recovered the existing results of some previous works. He also obtained sufficient conditions for linear stability in static and rigidly rotating columns for both inviscid and viscous fluids. El-Dib [14] has carried out the stability analysis of a rigidly rotating magnetic fluid column in the presence a periodic azimuthal magnetic field. His analytical results showed that the uniform magnetic field plays a stabilizing role and can be used to suppress the destabilizing influence of rotation, while the oscillating one plays a dual role in the stability criterion. El-Dib and Moatimid [15] and Moatimid and El-Dib [16] have developed a theoretical analysis to investigate the effect of periodic rotation of a cylindrical liquid jet under the influence of an axial and radial uniform electric field. Their analysis is based on the multiple time scales method. The analytical results in [15] show that the increase of the amplitude of the angular velocity has a destabilizing effect. They also found that the axial electric field plays a dual role in the stability criteria, a stabilizing influence in the non-resonance case and a destabilizing role in the resonance one. In [16], they showed that according to the periodicity of the unsteady rotation, the electric field changes its mechanism in the resonance case.

The phenomena of parametric resonance arise in many branches of physics and engineering. One of the important problems is that of dynamic instability which is the response of mechanical and elastic systems to time-varying loads, especially periodic loads. There are many cases in which the introduction of a small vibrational loading can stabilize a system which is statically unstable or destabilize a system that is statically stable. The treatment of the parametric excitation system having many degress of freedom and distinct natural frequencies is usually operated by using the multiple time scales as given by Nayfeh [17]. The behavior of such systems is described by an equation of the Hill or Mathieu types [18, 19]. It is well known that the stability of such solutions may be described by means of the characteristic curves of Mathieu functions which admit regions of resonance instability. The phenomena of interfacial stability in multilayer flow of viscoelastic fluids are of interest in many polymer processing applications, such as coextrusion of films and fibers. One major problem is the formation of interfacial waves which can result in a significant deterioration of product properties (i. e. mechanical, optical, etc). El-Dib and Motoog [20] investigated the stability of streaming in an electrified Maxwell fluid sheet. Their linear analysis resulted in coupled Mathieu equations. They found that the fluid sheet thickness plays a stabilizing role in the presence of a uniform electric field, while the damping role is observed for the resonance case.

In the present work, we extend the technique carried out by El-Dib [14] for rigidly rotating columns of a weakly viscoelastic fluid to include the presence of a surface current density on the fluid interface. The fluid column is held by capillary forces in the presence of an azimuthal periodic magnetic field. Therefore, we are concerned with the influence of surface currents on the stability of an azimuthal disturbance. The main

idea of this study is to indicate the relation between the presence of the surface current density and both the fluid viscoelastic parameters and the azimuthal magnetic field.

The plan of this work, which is of the Maxwell fluid instability type, is as follows: In Section 2, we give a description of the problems including the basic equations of the fluid mechanics and Maxwell's equations governing the motion of our model. This section contains also the appropriate boundary conditions and the corresponding solutions. Section 3 is devoted to the discussion of the case when no surface currents are present at the interface. In Secion 4, we analyse the viscoelastic conducting interface supporting surface currents.

2. Mathematical Formulation of the Problem

The motion of an infinitely long fluid column with low viscoelastic effects is considered. The fluid is assumed to have a viscoelastic nature described by the Maxwell constitutive relations. This column, having the density ρ_1 and magnetic permeability μ_1, performs a rigidly rotating motion, in a weightless condition, with a uniform angular velocity Ω_1 about its axis of symmetry. The fluid column is embedded in a rotating unbounded fluid having the density ρ_2, magnetic permeability μ_2 and a uniform angular velocity Ω_2. The two fluids are homogeneous and incompressible, and exhibit interfacial tension. The system is subjected to an azimuthal periodic magnetic field with a forcing frequency ω given by

$$\boldsymbol{H}_{0j} = H_j \cos\omega t\, \underline{e}_\theta, \quad j = 1, 2, \tag{2.1}$$

where $\underline{e}_\theta$ is the unit vector in the θ-direction.

In formulating Maxwell's relations, we assume that the magneto-quasistatic approximation is valid for the system [21]. Accordingly, Maxwell's equations may be reduced to

$$\nabla\cdot\mu\boldsymbol{H} = 0, \tag{2.2}$$

$$\nabla\times\boldsymbol{H} = \boldsymbol{J}_{\mathrm{f}}, \tag{2.3}$$

where $\boldsymbol{J}_{\mathrm{f}}$ represents the surface current density.

The equation which governs the behavior of Maxwell fluids [20] is given by

$$\rho\left[1+\lambda\left(\frac{\partial}{\partial t}+\boldsymbol{V}\cdot\nabla\right)\right]\left[\frac{\partial}{\partial t}\boldsymbol{V}+(\boldsymbol{V}\cdot\nabla)\boldsymbol{V}+\nabla P\right] = \eta\nabla^2\boldsymbol{V}, \tag{2.4}$$

with the incompressibility condition

$$\nabla\cdot\boldsymbol{V} = 0, \tag{2.5}$$

where $\boldsymbol{V}$ is the fluid velocity vector, P is the hydrostatic pressure, η the viscosity coefficient and λ the Maxwell relaxation time.

In order to make use of the domain perturbation technique, we confine the analysis to considering very weak viscoelastic effects which are belived to be significant only within a thin vortical surface layer, so that the motions in the bulk may be resonably assumed irrotational [20, 22]. Thus the derivations in this problem deal completely with potential flow so that the complicated manipulation of the boundary-layer equations for the weak vortical flow can be avoided. Since the field equation governing the irrotational flow is the Laplace equation, modifying the boundary conditions at the surface should be an acceptable means of including the small viscoelastic effects. Thus the viscoelastic effects are introduced through the normal damped stress term in the boundary condition at the surface of separation.

There are surface forces that must be accounted for by the stress tensor σ_{ij}:

The first is due to the magnetic forces as given by [23]

$$\boldsymbol{F} = \boldsymbol{J}_{\mathrm{f}}\times\mu\boldsymbol{H} - \frac{1}{2}\boldsymbol{H}\cdot\boldsymbol{H}\nabla\mu + \nabla\left(\frac{1}{2}\boldsymbol{H}\cdot\boldsymbol{H}\frac{\partial\mu}{\partial\rho}\rho\right). \tag{2.6}$$

The first term is the force resulting from a medium containing free surface currents $\boldsymbol{J}_{\mathrm{f}}$. It is the strongest magnetohydrodynamic term. The second term, called the magnetization force density, is due to inhomogenities in the magnetic material. The third term, called the magnetostriction term, being the gradient of a scalar quantity, is treated as a modification to the compressible fluid pressure and should be omitted from this analysis because of the incompressibility condition [23]. Manipulation of (2.6), which incorporates the irrotational nature of the magnetic field intensity, shows that the stress tensor representation of combined free surface currents and magnetization force densities is [21]

$$\pi_{ij} = \mu H_i H_j - \frac{1}{2}\mu H^2\delta_{ij}, \tag{2.7}$$

where δ_{ij} is the Kronecker's delta.

The other surface force results from the effect of the viscoelastisity. The rheologic behavior of the viscoelastic fluid of the Maxwell type may be obtained from the description

$$\left[1+\lambda\left(\frac{\partial}{\partial t}+\boldsymbol{V}\cdot\nabla\right)\right]\sigma_{rr}=2\eta\frac{\partial u}{\partial r}, \tag{2.8}$$

$$\left[1+\lambda\left(\frac{\partial}{\partial t}+\boldsymbol{V}.\nabla\right)\right]\sigma_{\theta\theta}=2\eta\left(\frac{u}{r}+\frac{1}{r}\frac{\partial v}{\partial\theta}\right), \tag{2.9}$$

$$\left[1+\lambda\left(\frac{\partial}{\partial t}+\boldsymbol{V}.\nabla\right)\right]\sigma_{r\theta}=\eta\left[\frac{1}{r}\frac{\partial u}{\partial\theta}+r\frac{\partial}{\partial r}\left(\frac{v}{r}\right)\right], \tag{2.10}$$

where

$$\sigma_{ij}=-P\delta_{ij}+\pi_{ij}. \tag{2.11}$$

Two dimensional cylindrical coordinates (r,θ) are used, so that u and v are the radial and azimuthal velocity components, respectively, of the fluid inside and outside the column.

2.1. Bulk Equations

In view of the weak viscoelastic approximation, which is considered here, the governing equations for the bulk of the fluid are

$$\frac{\partial u}{\partial t}+u\frac{\partial u}{\partial r}+\frac{v}{r}\frac{\partial u}{\partial\theta}-\frac{v^2}{r}=-\frac{1}{\rho}\frac{\partial P}{\partial r}, \tag{2.12}$$

$$\frac{\partial v}{\partial t}+u\frac{\partial v}{\partial r}+\frac{v}{r}\frac{\partial v}{\partial\theta}+\frac{vu}{r}=-\frac{1}{\rho r}\frac{\partial P}{\partial\theta}, \tag{2.13}$$

with the incompressibility condition

$$\frac{\partial u}{\partial r}+\frac{1}{r}\frac{\partial v}{\partial\theta}+\frac{u}{r}=0. \tag{2.14}$$

In accordance with the assumption that the fluid performs an irrotational motion, the velocity may be expressed as gradient of a velocity potential $\phi(r,\theta,t)$, with the incompressibility condition. This potential represents a solution of the Laplace equation

$$\nabla^2\phi(r,\theta,t)=0. \tag{2.15}$$

Due to the validly of the quasistatic approximation, a stream function ψ should be introduced such that

$$\boldsymbol{H}=\frac{1}{r}\frac{\partial\psi}{\partial\theta}\underline{e}_r-\frac{\partial\psi}{\partial r}\underline{e}_\theta, \tag{2.16}$$

where $\underline{e}_r$ is the unit vector in the radial direction. Clearly the stream function ψ guarantees that (2.2) is satisfied, while the remaining bulk equation ($\nabla\times\boldsymbol{H}=0$) shows that ψ obeyes the Laplace's equation

$$\nabla^2\psi(r,\theta,t)=0. \tag{2.17}$$

2.2. Surface Equations

If the position of the column surface is defined as $r=\xi(\theta,t)$, the equation of continuity for this surface is given by

$$u=\frac{\partial\xi}{\partial t}+\frac{v}{r}\frac{\partial\xi}{\partial\theta}. \tag{2.18}$$

There are two components for the magnetic surface equations:

The first component is due to the continuity of the normal component of the magnetic displacement, which leads to

$$n_r\|\mu H_r\|+n_\theta\|\mu H_\theta\|=0, \tag{2.19}$$

where n_r and n_θ are the radial and azimuthal components of the unit vector $\boldsymbol{n}$, respectively to the surface of separation, and the jump $\|\cdot\|$ is defined as $\|\cdot\|=(\cdot)^2-(\cdot)^1$. The second component is the continuity of the tangential component of the magnetic field, which gives

$$n_r\|H_\theta\|-n_\theta\|H_r\|=0. \tag{2.20}$$

The condition (2.20) is only valid if there are no free-surface currents present at the interface. Owing to the presence of surface currents on the column interface, the tangential component of the magnetic field is discontinuous. Instead, the continuity of the tangential stress is assumed [21].

At the boundary between the two fluid columns, $r=R$, two surface stress equations have to be satisfied:

The first corresponds to the continuity of the normal stress by the amount of the surface tension force, which gives

$$\boldsymbol{n}\cdot||\boldsymbol{F}|| = T\left(\frac{1}{R_1}+\frac{1}{R_2}\right), \tag{2.21}$$

where $\boldsymbol{F}$ is the total force acting on the interface, which is defined as

$$\boldsymbol{F} = (n_r, n_\theta)\begin{pmatrix}\sigma_{rr} & \sigma_{r\theta}\\ \sigma_{\theta r} & \sigma_{\theta\theta}\end{pmatrix}, \tag{2.22}$$

where the parameter T represents the surface tension coefficient, and R_1 and R_2 are the two principle radii of curvature. The second surface force corresponds to the continuity of the tangential stress, which leads to

$$\boldsymbol{n}\times||\boldsymbol{F}|| = \boldsymbol{0}. \tag{2.23}$$

2.3. Equilibrium Conditions

In the equlibrium state, we have the following configuration:

(i) The surface of separation is a cylinder of radius R.

(ii) The velocity profile becomes $\boldsymbol{v}^{(0)} = (0, r\Omega, 0)$.

(iii) The unit normal to interface is $\boldsymbol{n}^{(0)} = (1, 0, 0)$.

(iv) The principle radii of curvature are $R_1 = 1$ and $R_2 = 0$.

It follows that the equilibrium pressure yields

$$P_j^{(0)} = \frac{1}{2}\rho_j r^2\Omega_j^2 + \Upsilon_j(t), \quad j = 1, 2, \tag{2.24}$$

where the superscript (0) refers to the equilibrium state and $\Upsilon_j(t)$ is an arbitrary time-dependent function.

From the continuity of the normal stress tensor at the interface $r = R$, we get that the jump in pressure is zero, whence

$$\Upsilon_1(t) - \Upsilon_2(t) = \frac{T}{R} + \frac{1}{2}R^2(\rho_2\Omega_2^2 - \rho_1\Omega_1^2) - \frac{1}{2}(\mu_1 H_1^2 - \mu_2 H_2^2)\cos^2\omega t. \tag{2.25}$$

In equilibrium state, we shall be concerned with two cases:

(A) No free surface currents are present at the unperturbed interface.

(B) The viscoelastic conducting interface supports free surface currents.

Due to these assumptions, the jump in the tangential magnetic field will be zero in case A, so that $H_1 = H_2$, and this jump has a non-zero value in case B, so that

$$H_1 - H_2 = J_{\mathrm{f}}. \tag{2.26}$$

2.4. Linearized Equations of Motion

To perform a linear stability analysis of the considered system, the column radius will be assumed to be perturbed about its equilibrium value. The perturbed column radius is now becomes

$$r = R + \xi(\theta, t), \tag{2.27}$$

where

$$\xi(\theta, t) = \gamma(t)e^{im\theta}. \tag{2.28}$$

The arbitrary time dependent function $\gamma(t)$ represents the amplitude of the perturbation in the column radius, and the integer m is the azimuthal wavenumber. The limiting case of a very long longitudinal wavelength is considered here, so that the dependence of the variables on z can be neglected.

The bulk equations of motion and the surface equations mentioned above will be solved for these perturbations under the assumption that the perturbations are small, that is all equations (bulk and surface) will be linearized in the perturbed quantities before solving. The form of the azimuthal variation for all other perturbed variables will be the same as the dependence given in (2.28). To the first order, the unit normal to the column interface has the components $n_r = 1$ and $n_\theta = -r^{-1}\partial\xi/\partial\theta$. Accordingly, the linearized velocity potential ϕ and the stream function ψ are governed by the equations

$$\left(r^2\frac{\partial^2}{\partial r^2} + r\frac{\partial}{\partial r} - m^2\right)\phi = 0, \tag{2.29}$$

$$\left(r^2\frac{\partial^2}{\partial r^2} + r\frac{\partial}{\partial r} - m^2\right)\psi = 0, \tag{2.30}$$

while the increment of the pressure is given by

$$\pi(r,\theta,t) = -\rho\left(\frac{\partial\phi}{\partial t} - \frac{2i\Omega}{m}r\frac{\partial\phi}{\partial r} + im\Omega\phi\right). \quad (2.31)$$

Equation (2.29) may be solved under the kinematic boundary condition

$$\frac{\partial\phi_j}{\partial r} = \frac{\partial\xi}{\partial t} + im\Omega_j\xi, \quad (r = R). \quad (2.32)$$

Thus the velocity potential distribution ϕ_j, inside and outside the fluid column, respectively, are given by

$$\phi_1(r,\theta,t) = \frac{R}{m}\left(\frac{r}{R}\right)^m\left[\frac{\mathrm{d}\gamma}{\mathrm{d}t} + im\Omega_1\gamma\right]e^{im\theta}, \quad (2.33)$$

$$\text{if } r \le R,$$

$$\phi_2(r,\theta,t) = -\frac{R}{m}\left(\frac{R}{r}\right)^m\left[\frac{d\gamma}{dt} + im\Omega_2\gamma\right]e^{im\theta}, \quad (2.34)$$

$$\text{if } r \ge R.$$

In solving (2.30) with the appropriate boundary conditions, we shall deal with two cases, depending on whether or not the unperturbed interface supports free surface currents.

3. Case A: No Free Surface Currents Present at the Interface

In this case, we assume that the unperturbed interface supports no free surface currents, so that the magnetic field in the equilibrium configuration becomes $H_1 = H_2 = H_0$. However, the appropriate magnetic boundary conditions, which have to be satisfied at the surface $r = R$, are given by

(1.) The tangential component of the magnetic field should be continuous at the interface. This leads to

$$\frac{\partial\psi_1}{\partial r} - \frac{\partial\psi_2}{\partial r} = 0, \quad (3.1)$$

(2.) The normal component of the magnetic displacement is continuous at the interface, so that

$$\left(\mu_1\frac{\partial\psi_1}{\partial\theta} - \mu_2\frac{\partial\psi_2}{\partial\theta}\right) - \frac{\partial\xi}{\partial\theta}(\mu_1 - \mu_2)H_0\cos\omega t = 0. \quad (3.2)$$

With these boundary conditions, the solution of the Laplace equation (2.30) yields the following distributions of the stream function inside and outside the column:

$$\psi_1(r,\theta,t) = \left(\frac{\mu_1 - \mu_2}{\mu_1 + \mu_2}\right)\left(\frac{r}{R}\right)^m\gamma(t)H_0\cos\omega t\, e^{im\theta},$$

$$\text{if } r \le R, \quad (3.3)$$

$$\psi_2(r,\theta,t) = -\left(\frac{\mu_1 - \mu_2}{\mu_1 + \mu_2}\right)\left(\frac{R}{r}\right)^m\gamma(t)H_0\cos\omega t\, e^{im\theta},$$

$$\text{if } r \ge R. \quad (3.4)$$

It is well known that, for inviscid fluids, the jump in the tangential stress is equivalent to the continuity of the normal component of the magnetic field, since there are no free surface currents at the interface. That is in contrast with the presence of viscosity or viscoelasticity as considered here. Therefore, there exists a contribution for using this boundary condition now. Thus there are two remaining linearized boundary conditions given by the continuity of the tagential and normal stresses:

$$\frac{1}{r}\frac{\partial\xi}{\partial\theta}\left[(\sigma_{rr}^{(1)} - \sigma_{rr}^{(2)}) - (\sigma_{\theta\theta}^{(1)} - \sigma_{\theta\theta}^{(2)})\right] + (\sigma_{r\theta}^{(1)} - \sigma_{r\theta}^{(2)}) = 0, \quad (3.5)$$

$$\sigma_{rr}^{(1)} - \sigma_{rr}^{(2)} = -\frac{T}{r} + T\nabla^2\xi(\theta,t). \quad (3.6)$$

For the rheological behavior described above, the linearized tangential and normal stress components reduce, respectively, to

$$\left(\mu_1\frac{\partial\psi_1}{\partial\theta} - \mu_2\frac{\partial\psi_2}{\partial\theta}\right)H_0\cos\omega t \quad (3.7)$$

$$-\frac{\partial\xi}{\partial\theta}(\mu_1 - \mu_2)H_0^2\cos^2\omega t$$

$$+\eta_1\left[1 + \lambda_1\left(\frac{\partial}{\partial t} + \Omega_1\frac{\partial}{\partial\theta}\right)\right]^{-1}\frac{\partial}{\partial\theta}\left(\frac{\partial\phi_1}{\partial r} - \frac{\phi_1}{r}\right)$$

$$-\eta_2\left[1 + \lambda_2\left(\frac{\partial}{\partial t} + \Omega_2\frac{\partial}{\partial\theta}\right)\right]^{-1}\frac{\partial}{\partial\theta}\left(\frac{\partial\phi_2}{\partial r} - \frac{\phi_2}{r}\right) = 0,$$

and

$$\pi_1 - \pi_2 = R(\rho_2\Omega_2^2 - \rho_1\Omega_1^2)\xi + \frac{T}{R^2}(m^2-1)\xi \quad (3.8)$$
$$- \left(\mu_1\frac{\partial\psi_1}{\partial r} - \mu_2\frac{\partial\psi_2}{\partial r}\right) H_0\cos\omega t$$
$$+ \eta_1\left[1+\lambda_1\left(\frac{\partial}{\partial t}+\Omega_1\frac{\partial}{\partial\theta}\right)\right]^{-1}\frac{\partial^2\phi_1}{\partial r^2}$$
$$- \eta_2\left[1+\lambda_2\left(\frac{\partial}{\partial t}+\Omega_2\frac{\partial}{\partial\theta}\right)\right]^{-1}\frac{\partial^2\phi_1}{\partial r^2}.$$

These conditions are used to determine the dispersion equation that describes the behavior of the surface wave. Substituting both the stream function $\psi_j(r,\theta,t)$ and the velocity potential $\phi_j(r,\theta,t)$ from (2.33), (2.34), (3.3) and (3.4), and then using the binomial expansion to write the elastic operator as

$$\left[1+\lambda\left(\frac{\partial}{\partial t}+\Omega\frac{\partial}{\partial\theta}\right)\right]^{-1} \cong 1-\lambda\left(\frac{\partial}{\partial t}+\Omega\frac{\partial}{\partial\theta}\right)+\ldots,$$

(3.7) and (3.8) become

$$\left[\eta_2\lambda_2(m+1)-\eta_1\lambda_1(m-1)\right]\frac{\mathrm{d}^2\gamma}{\mathrm{d}t^2} \quad (3.9)$$
$$+\left[-\left(\eta_2(m+1)-\eta_1(m-1)\right)+2im\left(\eta_2\lambda_2\Omega_2(m+1)\right.\right.$$
$$\left.\left.-\eta_1\lambda_1\Omega_1(m-1)\right)\right]\frac{\mathrm{d}\gamma}{\mathrm{d}t}$$
$$-\left[m^2\left(\eta_2\lambda_2\Omega_2^2(m+1)-\eta_1\lambda_1\Omega_1^2(m-1)\right)\right.$$
$$\left.+im\left(\eta_2\Omega_2(m+1)-\eta_1\Omega_1(m-1)\right)\right]\gamma=0$$

and

$$\left[R^2(\rho_1+\rho_2)-2m\left(\eta_1\lambda_1(m-1)\right.\right. \quad (3.10)$$
$$\left.\left.+\eta_2\lambda_2(m+1)\right)\right]\frac{\mathrm{d}^2\gamma}{\mathrm{d}t^2}$$
$$+\left[2m\left(\eta_2(m+1)+\eta_1(m-1)\right)\right.$$
$$+2iR^2\left(\rho_2\Omega_2(m+1)+\rho_1\Omega_1(m-1)\right)$$
$$\left.-2im^2\left(\eta_2\lambda_2\Omega_2(m+1)+\eta_1\lambda_1\Omega_1(m-1)\right)\right]\frac{\mathrm{d}\gamma}{\mathrm{d}t}$$
$$+\left[\frac{m(m^2-1)T}{R}-mR^2\left(\rho_2\Omega_2^2(m+1)+\rho_1\Omega_1^2(m-1)\right)\right.$$
$$+2m^3\left(\eta_2\lambda_2\Omega_2^2(m+1)+\eta_1\lambda_1\Omega_1^2(m-1)\right)$$
$$+2im^2\left(\eta_2\Omega_2(m+1)+\eta_1\Omega_1(m-1)\right)$$
$$\left.+m^2\mu^*H_0^2\cos^2\omega t\right]\gamma=0,$$

where $\mu^* = (\mu_2-\mu_1)^2/(\mu_2+\mu_1)$.

3.1. Characteristic Equation

In deriving the characteristic equation, we must combine (3.9) and (3.10) to a single equation. The elimination of the real part of the damping term between these equations, leads to a single equation of the Mathieu type with an imaginary damping term. This equation represents the dispersion equation which controls the behavior of viscoelastic effects on the surface waves instability.

It is convenient here to write the dispersion equation in an appropriate dimensionless form. This can be done in a number of ways, depending primarily on the choice of the characteristic length L. Consider the following dimensionless forms: The characteristic length $L=\sqrt{\eta_2\lambda_2/\rho_2}$, the characteristic time $t=\lambda_2$, and the characteristic mass $M=\eta_2\lambda_2\sqrt{\eta_2\lambda_2/\rho_2}$. The other dimensionless quantities are given by $R=R^*\sqrt{\eta_2\lambda_2/\rho_2}$, $\omega=\omega^*/\lambda_2$, $\Omega_j=\Omega_j^*/\lambda_2$, $H^2=H^{*2}\eta_2/\lambda_2$, $t=t^*\lambda_2$ and $T=T^*\eta_2\sqrt{\eta_2/\rho_2\lambda_2}$. The star may be dropped later for simplicity. For this stage, the dispersion relation becomes

$$\frac{\mathrm{d}^2\gamma}{\mathrm{d}t^2}+2i\alpha\frac{\mathrm{d}\gamma}{\mathrm{d}t}+(\delta-\alpha^2+QH_0^2\cos^2 wt+i\beta)\gamma=0, \quad (3.11)$$

where

$$\alpha=\left[R^2[\Omega_2(m+1)+\rho\Omega_1(m-1)](m+1-\eta(m-1))\right.$$
$$+m^2[\Omega_2(m+1)-\lambda\eta\Omega_1(m-1)]$$
$$\cdot(m+1+\eta(m-1))$$
$$\left.+2\eta m^2(m^2-1)(\Omega_2-\lambda\Omega_1)\right]/\Delta,$$

$$\delta-\alpha^2=m\left[\frac{T}{R}(m^2-1)(m+1-\eta(m-1))\right.$$
$$+4\eta m^2(m^2-1)(\lambda\Omega_1^2-\Omega_2^2)-R^2[\Omega_2^2(m+1)$$
$$\left.+\rho\Omega_1^2(m-1)](m+1-\eta(m-1))\right]/\Delta,$$

$$Q = \frac{\mu^* m^2(m+1-\eta(m-1))}{\Delta},$$

$$\beta = \frac{4\eta m^2(m^2-1)(\Omega_1-\Omega_2)}{\Delta},$$

$$\Delta = R^2(1+\rho)(m+1) - \eta(m-1)) + 4\eta(m^2-1)(1-\lambda),$$

$$\rho = \frac{\rho_1}{\rho_2},\ \lambda = \frac{\lambda_1}{\lambda_2} \text{ and } \eta = \frac{\eta_1}{\eta_2}.$$

The canonical normal form of equation (3.11) may be obtained by the transformation

$$\gamma(t) = \Gamma(t)\exp(-i\alpha t), \tag{3.12}$$

to yield

$$\frac{\mathrm{d}^2\Gamma}{\mathrm{d}t^2} + (\delta + QH_0^2\cos^2\omega t + i\beta)\Gamma = 0, \tag{3.13}$$

which is a second order differential equation of Mathieu type with complex coefficient. In the limiting case for a non-rotating fluid column, this equation reduces to the standard form of the Mathieu equation with real coefficients.

Inspection of Mathieu equation (3.13), we observe that the considered system produces a singlularity, which arises when the radius R tends to the critical value R_c, where

$$R_c^2 = \frac{4m\eta(m^2-1)(\lambda-1)}{(1+\rho)(m+1-\eta(m-1))}. \tag{3.14}$$

A resonance case will appear in the neighbourhood of the value of R_c. In a pure viscous flow, a viscous resonance occurs near the critical value $\eta_c = \frac{m+1}{m-1}$ [6].

3.2. Stability Analysis within the Marginal State

In order to analyze the stability of the Mathieu equation (3.13), we shall be interested in the examination of the marginal stability as a first scope. This marginal state deals with the periodic solution of this equation. The condition satisfying the marginal state is actually associated with the vanishing of the coefficient β, or is trivially satisfied for inviscid fluids. This has been already discussed by El-Dib [14]. For a non-vanishing viscosity, the parameter β vanishes under a certain condition. This condition arises when the two fluids columns rotate with the same angular velocity, i. e. $\Omega_1 = \Omega_2 = \Omega$ for all azimuthal wavenumber m.

At this stage, the characteristic equation which governs the surface wave for the marginal state is given by

$$\frac{\mathrm{d}^2\Gamma}{\mathrm{d}t^2} + (\delta + QH_0^2\cos^2\omega t)\Gamma = 0. \tag{3.15}$$

In dealing with the case of a uniform magnetic field, the field frequency ω approaches zero into (3.15). Therefore the solution of the resulting characteristic equation has an exponential form. The stability criterion then becomes

$$\delta + QH_0^2 > 0. \tag{3.16}$$

In the absence of the magnetic field, the stability condition reduces to $\delta > 0$, while the presence of the uniform magnetic field yields the condition

$$\begin{aligned} H_0^2 &> -\frac{\delta}{Q}, \quad \text{provided} \quad Q > 0, \\ H_0^2 &< -\frac{\delta}{Q}, \quad \text{provided} \quad Q < 0. \end{aligned} \tag{3.17}$$

If $Q > 0$, the stability condition (3.16) is trivially satisfied for positive values of δ (which occurs in the case of pure viscous fluids), while the stabilizing influence of the magnetic field appears as $\delta Q < 0$. The transition curve, sparating the stable region from the unstable one, becomes

$$H_0^2 > H_0^* = -\frac{\delta}{Q}. \tag{3.18}$$

It is worthwhile to observe that there exists a viscoelastic sigularity when determining the transition curve H_0^*. This is due to the change in the curve H_0^*. Thus there exists an instability zone in the neighborhood of the value of the critical R_c. Note that this viscoelastic singularity can be excluded when both fluid columns have the same relaxation time $\lambda = 1$. In this case, the system behaves like a pure viscous flow. This shows a stability influence, that appears at the singularity due to the variation of the relaxation time and it can be suppressed as $\lambda = 1$.

In the case of a non-vanishing field frequency ω, the stability arises whence the following inequality is satisfied:

$$H_0^4Q^2 + 16(\omega^2-\delta)QH_0^2 + 32\delta(\omega^2-\delta) > 0. \tag{3.19}$$

This stability criterion yields the bounded regions of the solutions of the Mathieu equation (3.15) as given by Mohamed and Nayyer [24]. It is observed that this condition is satisfied as $\omega^2 \geq \delta$; $\delta > 0$, for arbitrary Q or H_0^2.

In terms of the magnetic field H_0^2, the stability condition (3.19) takes the form

$$(H_0^2 - H_1^*)(H_0^2 - H_2^*) > 0, \tag{3.20}$$

where

$$H_{1,2}^* = \frac{8}{Q}\left\{-(\omega^2 - \delta) \pm \sqrt{(\omega^2 - \delta)\left(\omega^2 - \frac{3}{2}\delta\right)}\right\}. \tag{3.21}$$

Clearly H_1^* and H_2^* have real values, whence the field frequency ω satisfies the relation

$$\delta > \omega^2 > \frac{3}{2}\delta. \tag{3.22}$$

It follows that the transition curves $H_{1,2}^*$ should be bounded by an unstable region as condition (3.22) holds. Therefore the stable regions are characterized by the conditions

$$H_0^2 > H_1^* \text{ and } H_0^2 < H_2^*, \ (H_1^* > H_2^*). \tag{3.23}$$

The two transition curves H_1^* and H_2^* will meet when the column radius is R_c. Another intersection for the two transition curves occurs when the field frequency ω^2 has the value δ. Since the parameter $\sqrt{\delta}$ represents the disturbance frequency of the Mathieu equation (3.15) as $H_0^2 = 0$, and the nearness of ω to $\sqrt{\delta}$ produces the reasonance case. Hence a coupled reasonance point occurs at

$$\omega = \sqrt{\delta} \text{ as } R = R_c. \tag{3.24}$$

It is useful to investigate the transition curves which separate stable from unstable regions in non-dimensional form as stated in Section 3.1. Therefore, in this section the goal is to calculate stable profiles in case of a uniform magnetic field as well as an oscillating one. In order to examine the influence of uniform fields on the stability criteria, numerical calculations for the stability condition (3.18) were made. The results of the calculations are displayed in the log H_0^2 vs. log R plane in Figs. 1 and 2. It is apparent from these figures that an increase in the magnetic field H_0^2 as well as the column radius R has a stabilizing influence. This stabilizing role is diminished by an increase of both the angular velocity Ω and the azimuthal wavenumber m. Figure 1 is computed for $\Omega = 5$ and values of m from 1 to 4. It is readily seen that intersections indicate the dual role of the azimuthal wavenumber in the stability criterion. For small values of R, m has a destabilizing influence, and vice versa. Figure 2 pictures for $m = 1$ various values of the angular velocity Ω. It is evident that an increase of Ω increases the unstable regions, which shows the destabilizing influence of rotation.

In order to examine of the influence of the oscillating field on the stability, numerical calculations for the stability condition (3.20) are made. These calculations are displayed in the log H_0^2 vs. log R plane in Figs. 3 and 4. In Fig. 3, the same influence of rotation, given above in the case of a uniform field, is also obtained in the case of a periodic field. This shows that the destablizing influence of the rotation does not depend on the mechanism of the field. In Fig. 4, the stabilizing influence of a periodicity force is readily seen. In these figures, one branch of the transition is only computed while the other one has negative values and hence has no implication on the stability analysis.

3.3. Resonance Mechanism and a Growth Rate Solution of the Mathieu equation (3.13)

As the coefficient β has a non-zero value in (3.13), a growth rate solution is presented. A stability description for (3.13) was made by El-Dib [14]. He used the method of multiple time scales to analyze a similar equation. The treatment was made for two time scales T_0 and T_1 as fast and slow time-scales, respectively. This analysis has shown that the growth rate for the zero-order solution is given by

$$\Gamma_0(T_0, T_1) = \Gamma(T_1)\exp[(\sigma + i\omega_0)T_0] + \text{c.c.}, \tag{3.25}$$

where $\Gamma(T_1)$ is an unknown complex function, c.c. represents the complex conjugate of the preceeding terms, σ and ω_0 are real. Both σ and ω_0 are satisfied by the equations

$$\sigma^2 - \omega_0^2 + \delta = 0, \text{ and } 2\sigma\omega_0 + \beta = 0. \tag{3.26}$$

Elimination of the parameter σ yields

$$\omega_0^2 = \frac{1}{2}\left(\delta + \sqrt{\sigma^2 - \beta^2}\right). \tag{3.27}$$

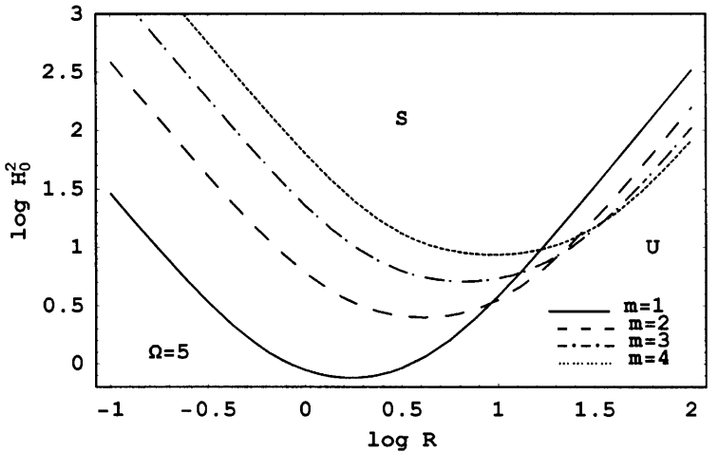

Fig. 1. Stability diagram for a system having: ρ = 0.77, λ = 1, Ω = 5, η = 0.67, T = 35 and μ = 200. The figure indicates the transition curve H_0^* given by (3.18). The region labeled S is the stable region, while the region labeled U denotes the unstable one.

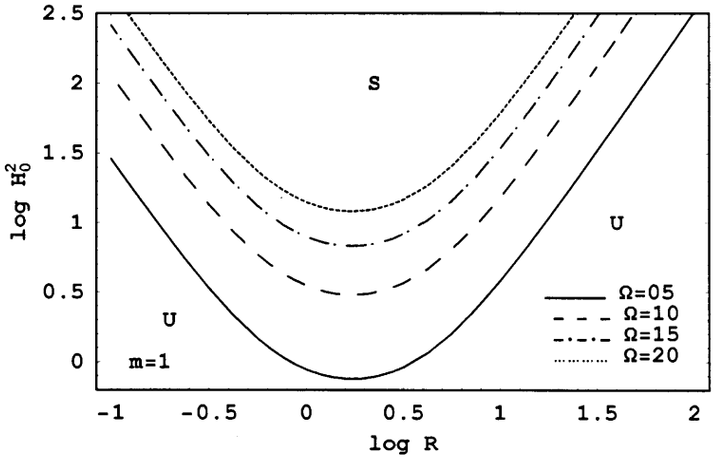

Fig. 2. Stability diagram for the same system as in Fig. 1, but for a single value of m and various values of Ω.

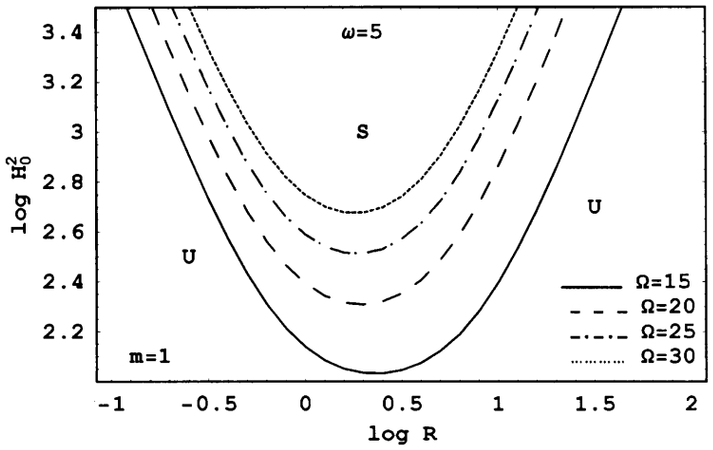

Fig. 3. Stability diagram for the same system as in Fig. 2 but for ω = 5 and different values of Ω. The graph indicates the transition curve H_1^* given by (3.21), while the transition curve H_2^* has negative values.

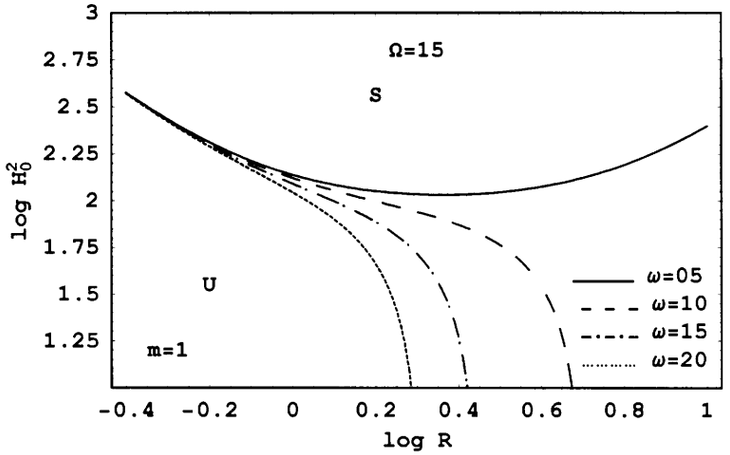

Fig. 4. Stability diagram for the same system as in Fig. 3 but for Ω = 15 and different values of ω.

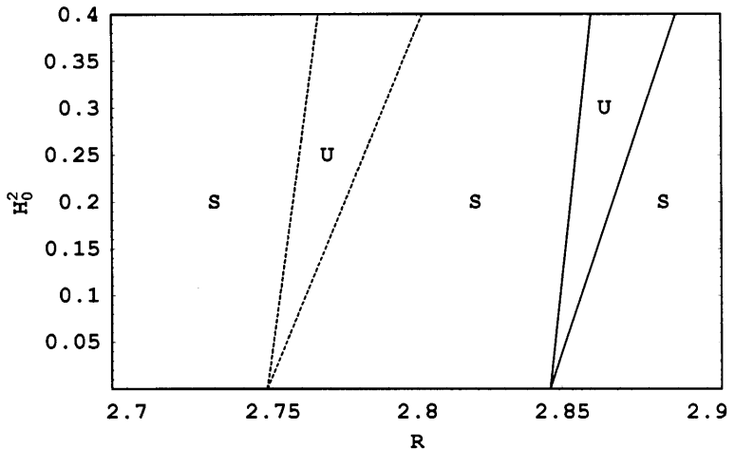

Fig. 5. Stability diagram of the system as in Fig. 1, but for m = 1, Ω_2 = 8; Ω_1 = 3 (solid lines) and Ω_1 = 8 (dotted lines). The graph indicates the transition curves H_1^{**} and H_2^{**} given in (3.30) and (3.31).

In the resonance case of nearness of the field frequency ω to the distrubance frequency ω_0, the stability conditions are given by

$$\omega > \omega_0 + \frac{QH_0^2}{8\sqrt{\delta^2-\beta^2}}\left[2\omega + \sqrt{3\delta - 2\omega_0^2}\right], \quad (3.28)$$

$$\omega < \omega_0 + \frac{QH_0^2}{8\sqrt{\delta^2-\beta^2}}\left[2\omega - \sqrt{3\delta - 2\omega_0^2}\right], \quad (3.29)$$

provided that the criteria of stability, in the zero-order case are satisfied, i.e.

$$\delta > 0, \text{ and } \delta > \beta. \quad (3.30)$$

Clearly the resonance point, which is presented at $\omega = \omega_0$, occurs if $H_0 = 0$ or $\eta = \frac{m+1}{m-1}$.

The transition curves separating the stable from the unstabl region, in terms of the magnetic field intensity H_0^2, are

$$H_0^2 = H_1^{**} = \frac{8(\omega-\omega_0)(\delta^2-\beta^2)^{1/2}}{Q\left(2\omega_0 + (3\delta - 2\omega_0^2)^{1/2}\right)}, \quad (3.31)$$

$$H_0^2 = H_2^{**} = \frac{8(\omega-\omega_0)(\delta^2-\beta^2)^{1/2}}{Q\left(2\omega_0 - (3\delta - 2\omega_0^2)^{1/2}\right)}. \quad (3.32)$$

According to the Floquet theory [17], the parameter space contains stable and unstable parts. The region bounded by the transition curves H_1^{**} and H_2^{**} is the unstable region, while the area outside these curves is the stable one. The width of the unstable region is represented by $H_1^{**} - H_2^{**}$. An increase of this width indicates the destabilizing influence, while its decrease represents a stabilizing role. The numerical calculations for the transition curves H_1^{**} and H_2^{**} (the solid and dotted lines) in the resonance case of ω_0 near ω are displayed in Figure 5. In this graph H_0^2 is plotted versus the column radius R. The solid curves correspond to Ω_1 = 3 and Ω_2 = 8, while the dotted ones correspond to $\Omega_1 = \Omega_2$ = 8. The resonance of the dotted lines occurs at R = 2.74819. The graph shows that the resonance region of the solid lines is slightly shifted to the right, so that the resonance point occurs at R = 2.84588.

4. Case B: Viscoelastic Conducting Interface Supporting Free Surface Currents

In this section, the stability analysis has been carried out for a rheological behavior of the viscoelastic interface in the presence of free surface currents. The presence of free surface currents J_f on the interface $r = R$, leads to $||H|| \neq 0$, so that the magnetic conditions at the interface are as follows:

Due to the presence of surface currents, the continuity of the tangential stress (2.23) is applicable, while the continuity of the normal component of the magnetic field (2.19) still holds. Applying these boundary conditions with the solution of the Laplace equation (2.17), keeping in mined that $H_1 \neq H_2$, we obtain

$$\psi_1(r,\theta,t) = \frac{1}{m\mu_1(H_2-H_1)\cos\omega t}\left(\frac{r}{R}\right)^m \quad (4.1)$$

$$\cdot\left\{2i\left[\eta_1(m-1)\left(1-\lambda_1\left(\frac{\mathrm{d}}{\mathrm{d}t} + im\Omega_1\right)\right)\right.\right.$$

$$-\eta_2(m+1)\Big(1-\lambda_2\Big(\frac{\mathrm{d}}{\mathrm{d}t}+im\Omega_2\Big)\Big)\Big]\frac{\mathrm{d}\gamma}{\mathrm{d}t}$$

$$-m\Big[2\eta_1\Omega_1(m-1)\Big(1-\lambda_1\Big(\frac{\mathrm{d}}{\mathrm{d}t}+im\Omega_1\Big)\Big)$$

$$-2\eta_2\Omega_2(m+1)\Big(1-\lambda_2\Big(\frac{\mathrm{d}}{\mathrm{d}t}+im\Omega_2\Big)\Big)$$

$$+i\mu_1H_1(H_1-H_2)\cos^2\omega t\Big]\gamma\Big\}e^{im\theta},\ (r\le R),$$

$$\psi_2(r,\theta,t)=\frac{-1}{m\mu_2(H_2-H_1)\cos\omega t}\left(\frac{R}{r}\right)^m \tag{4.2}$$

$$\cdot\Big\{2i\Big[\eta_1(m-1)\Big(1-\lambda_1\Big(\frac{\mathrm{d}}{\mathrm{d}t}+im\Omega_1\Big)\Big)$$

$$-\eta_2(m+1)\Big(1-\lambda_2\Big(\frac{\mathrm{d}}{\mathrm{d}t}+im\Omega_2\Big)\Big)\Big]\frac{\mathrm{d}\gamma}{\mathrm{d}t}$$

$$-m\Big[2\eta_1\Omega_1(m-1)\Big(1-\lambda_1\Big(\frac{\mathrm{d}}{\mathrm{d}t}+im\Omega_1\Big)\Big)$$

$$-2\eta_2\Omega_2(m+1)\Big(1-\lambda_2\Big(\frac{\mathrm{d}}{\mathrm{d}t}+im\Omega_2\Big)\Big)$$

$$+i\mu_2H_2(H_1-H_2)\cos^2\omega t\Big]\gamma\Big\}e^{im\theta},\ (r\ge R).$$

It is clear that the stream function ψ is affected by the column radius, the angular velocity, the viscosity, the elasticity and the magnetic field.

Consider the equilibrium configuration

$$H_1=\left(\frac{H}{H-1}\right)J_{\mathrm{f}},\ H_2=\left(\frac{1}{H-1}\right)J_{\mathrm{f}}, \tag{4.3}$$

where H is the stratified magnetic field intensity $\frac{H_1}{H_2}$. Using the same dimensionless quantities as in case A, the amplitude equation for the surface waves can be achieved to take the form

$$\frac{\mathrm{d}^2\gamma}{\mathrm{d}t^2}+2(a_1+ib_1)\frac{\mathrm{d}\gamma}{\mathrm{d}t}$$

$$+(a_2+qJ_{\mathrm{f}}^2\cos^2\omega t+2ib_2)\gamma=0, \tag{4.4}$$

which is a damping second-order equation of Mathieu type with complex coefficients. These coefficients are given as

$$a_1=\frac{2m[H(m+1)-\eta(m-1)]}{\Pi},$$

$$b_1=\big\{R^2(H-1)[\Omega_2(m+1)+\rho\Omega_1(m-1)]$$

$$-4m^2[\Omega_2H(m+1)-\eta\lambda\Omega_1(m-1)]\big\}/\Pi,$$

$$a_2=m(H-1)\Big\{\frac{T}{R}(m^2-1)$$

$$-R^2[\Omega_2^2(m+1)+\rho\Omega_1^2(m-1)]$$

$$+\frac{4m^2}{(H-1)}[\Omega_2^2H(m+1)-\eta\lambda\Omega_1^2(m-1)]\Big\}/\Pi,$$

$$q=\frac{m^2(\mu_1H^2+\mu_2)}{(H-1)\Pi},$$

$$b_2=2m^2[\Omega_2H(m+1)-\eta\Omega_1(m-1)]/\Pi,$$

and

$$\Pi=R^2(\rho+1)(H-1)$$

$$-4m[H(m+1)-\lambda\eta(m-1)].$$

If the above characteristic equation, which is governed by the Mathieu equation (4.4), has a growth rate disturbance of the form $\exp(\sigma^*+i\omega^*)t$. The stability depends on the sign of the real part σ^*. If it is positive, then the amplitude of the distrubance grows with time and the motion becomes unstable, if it is negative, the motion is stable and if it is zero, the marginal stability arises.

Before we proceed to the general case, it is interesting to discuss some special cases:

4.1. Stability Behavior of a Viscoelastic Column without Rotation

In the absence of rotation, the dispersion relation becomes

$$\frac{\mathrm{d}^2\gamma}{\mathrm{d}t^2}+2a_1\frac{\mathrm{d}\gamma}{\mathrm{d}t}+(a_{20}+qJ_{\mathrm{f}}^2\cos^2\omega t)\gamma=0, \tag{4.5}$$

where

$$a_{20}=\frac{Tm}{\Pi R}(m^2-1)(H-1).$$

This is a damped Mathieu equation with real coefficients. It is clear that there is a critical value for the stratified magnetic field for which the damping term is absent; this critical value is given by

$$H_c = \frac{\eta(m-1)}{m+1}. \tag{4.6}$$

In the case of a uniform magnetic field, the stability analysis of (4.5) imposes the conditions

$$\begin{aligned} J_f^2 &> J^* \quad \text{provided} \quad q > 0 \\ J_f^2 &< J^* \quad \text{provided} \quad q < 0 \end{aligned} \tag{4.7}$$

where $J^* = (a_1^2 - a_{20})/q$.

It is easy to show that for negative values of J^* the first condition is trivially satisfied and the free surface currents have no implication for the stability, while the second one is false and then instability is present. In order to perform a numerical approach to the linear stability of the wave propagation on the interface, it is useful to investigate the transition curves given by the inequalities (4.7). Therefore, some chosen example is considered in dimensionless forms, where the results for the calculations, displayed in the J_f^2 vs. R plane in Fig. 6, indicate the influence of the parameter λ on the stability of the system.

In the presence of the field frequency ω, the stability picture changes dramatically. Grimshaw [25] has examined the Mathieu equation (4.5) by a perturbation technique. On the boundaries of the first unstable region in the Mathieu diagram there is a periodic solution with period 2π. The stability condition is thus described by

$$(J_f^2 - J_1^*)(J_f^* - J_2^*) > 0. \tag{4.8}$$

Thus the stability criterion reduces to

$$J_f^2 > J_1^* \text{ or } J_f^2 < J_2^*;\ J_1^* > J_2^*, \tag{4.9}$$

where

$$J_{1,2}^* = \frac{4}{3q}\left\{2(\omega^2 - a_{20}) \pm \sqrt{(\omega^2 - a_{20})^2 - 12a_1^2\omega^2}\right\}$$

are the transition curves separating the stable region from the unstable region. The two transition curves (4.9), obtained by numerical calculations, are displayed in Figs. 7 - 9. Figure 7 illustrates the case where $m = 1$, $R = 5$ and $\omega = 20$. It is found that, if H increases, two unstable resonance regions, bounded by stable regions appear, the width of which increases with the surface current J_f^2. The decrease of J_f^2 has a stabilizing influence. In this graph, two resonance points are found. One of them meets the H-axis at $H = 1$, while the other one lies above the H-axis. As indicated in Fig. 8, these two resonance points coincide at $H = 1$ if $\rho = 0.5$, $\lambda = 2$, $\eta = 1.67$, $R = 40$ and $\omega = 10$. The intersection of the transition curves J_1^* and J_2^* at $H = 1$ corresponds to zero surface current density. This agrees with case A in which $H_1 = H_2$ as discussed before. In Fig. 9, we have repeated the above calculations for several values of the field frequency ω. It is seen that, as ω is increased, the unstable region decreases in width to cause an increase in the stable area. It follows that the field frequency has a stabilizing influence.

4.2. The Marginal State Analysis

Equation (4.4) represents the Mathieu equation with damped terms. This equation has a growth rate solution, the stability analysis being rather complex. To economize this complexity, we shall construct the stability configuration through the marginal state. Thus we shall be concerned with the periodic solutions for this equation. To accomplish this marginal state, two conditions must be satisfied: The necessary and sufficient conditions of stability are, respectively,

$$\frac{d^2\gamma}{dt^2} + 2ib_1\frac{d\gamma}{dt} + (a_2 + qJ_f^2\cos^2\omega t)\gamma = 0 \tag{4.10}$$

and

$$a_1\frac{d\gamma}{dt} + ib_2\gamma = 0. \tag{4.11}$$

It is worthwhile to observe that the equation governing the marginal state can be formulated by combining the necessary condition (4.10) with the sufficient condition (4.11) into a single condition. To do this, we must distinguish between two cases for the validly of the sufficient condition (4.11): The first case deals with the non-vanishing of the coefficients a_1 and b_2. The second deals with the vanishing of these coefficients.

4.2.1. The combination between the necessary and sufficient conditions

The assumption that the coefficients a_1 and b_2 are non-zero allows us to use (4.11) to remove the

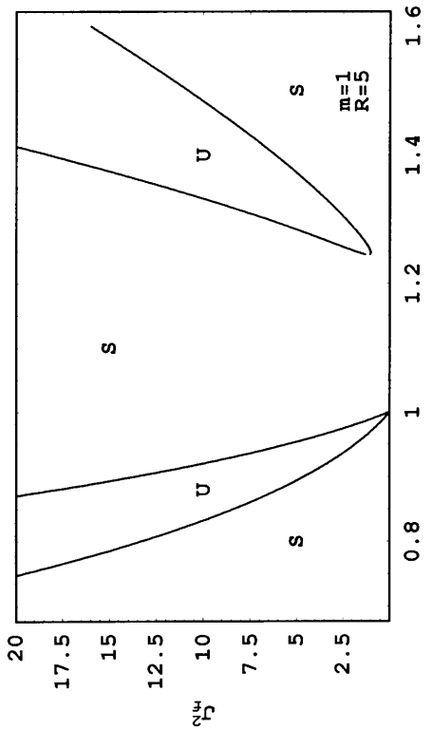

Fig. 6. Stability diagram for a system having: $\rho = 0.77$, $\eta = 0.67$, $T = 35$, $\mu_1 = 80.34$, $\mu_2 = 70.23$ and $m = 2$, $H = 5$, $\Omega_1 = \Omega_2 = 0$ and for various values of the parameter λ. The figure indicates the transition curves given in (4.7).

Fig. 7. Stability diagram for the same system as considered in Fig. 6, but when $\lambda = 1$, $m = 1$, $R = 5$ and $\omega = 20$. The graph indicates the transition curves given in the inequalities (4.9).

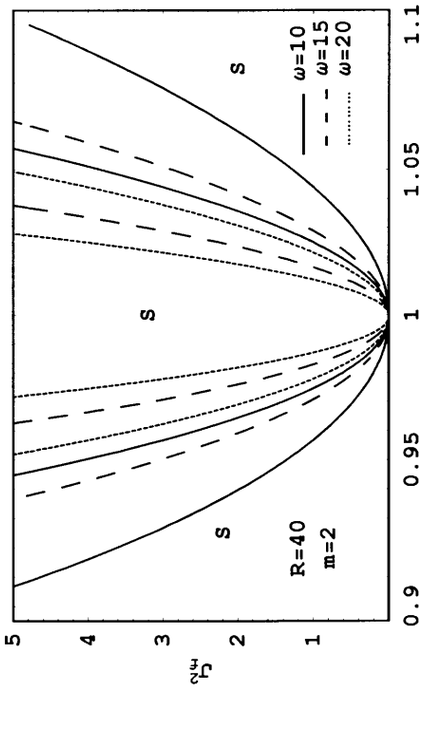

Fig. 9. Stability diagram for the same system as considered in Fig. 8, but for various values of ω.

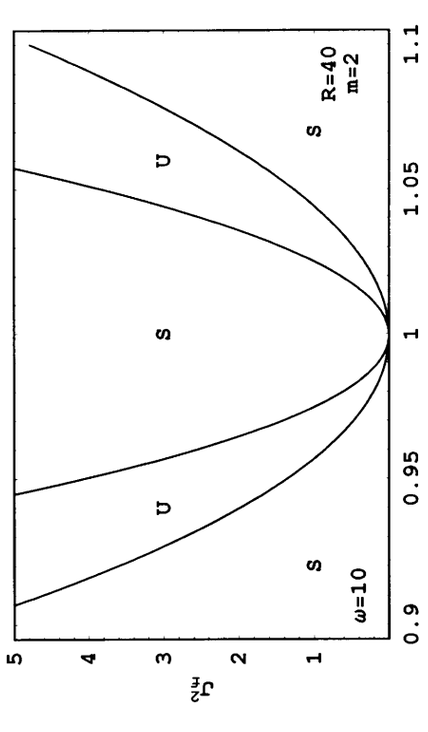

Fig. 8. Stability diagram for the same system as considered in Fig. 7, but when $R = 40$, $\lambda = 2$, $\eta = 1.67$, $m = 2$, $\omega = 10$ and $\rho = 0.5$.

damping term from (4.10). At this stage, the necessary and sufficient conditions for the marginal state are governed by the Mathieu equation

$$\frac{\mathrm{d}^2\gamma}{\mathrm{d}t^2}+\left[\frac{1}{a_1}(a_1a_2+2b_1b_2)+qJ_{\mathrm{f}}^2\cos^2\omega t\right]\gamma=0, \quad (4.12)$$

$a\neq 0$.

For a static magnetic field $\omega\to 0$, the stability condition reduces to

$$J_{\mathrm{f}}^2>J^{**} \text{ or } J_{\mathrm{f}}^2<J^{**}, \quad (4.13)$$

depending on the sign of q,

where

$$J^{**}=-\frac{1}{a_1q}(a_1a_2+2b_1b_2).$$

In order to screen the examination of the influence of the uniform field on the stability criteria, numerical calculations for the stability condition (4.13) were made. The results for the calculations are displayed in Figs. 10 and 11 in the J_{f}^2 vs. H plane. The calculations showed that $q<0$, thus stability, occurs when $J_{\mathrm{f}}^2<J^{**}$. Figures 10 and 11 drawn to indicate the role of the angular velocities on the stability picture. We see that stability is not possible when $H<1$. For $H>1$, the system may be stable for surface currents, J_{f}^2, less than J^{**} for a given H. This means that the surface currents have a destabilizing influence as does the normal field on the inviscid fluid. It is found that the stability increases for larg values of $\mid \Omega_1-\Omega_2 \mid$, especially at large values of H.

In the presence of the field frequency ω, as discussed before, the stability conditions may be expressed as

$$J_{\mathrm{f}}^2>J_1^{**} \text{ and } J_{\mathrm{f}}^2<J_2^{**};\ J_1^{**}>J_2^{**}, \quad (4.14)$$

where

$$J_{1,2}^{**}=\frac{8}{q}\Bigg[-\left(\omega^2-\frac{1}{a_1}(a_1a_2+2b_1b_2)\right)\mp\left(\omega^2-\frac{1}{a_1}(a_1a_2+2b_1b_2)\right)^{\frac{1}{2}}\cdot\left(\omega^2-\frac{3}{2a_1}(a_1a_2+2b_1b_2)\right)^{\frac{1}{2}}\Bigg].$$

4.2.2. The contribution for vanshing the sufficient condition (4.11)

This is the second interesting case for deriving the marginal stability. The analysis deals with the vanshing of the coefficients a_1 and b_1 of the sufficient condition (4.6). This is satisfied if

$$H=\frac{\eta(m-1)}{m+1} \text{ and } \Omega_1=\Omega_2=\Omega. \quad (4.15)$$

Introducing the transformation

$$\gamma(t)=\Psi(t)\exp(-ib_1t), \quad (4.16)$$

$\Psi(t)$ represents a time dependent amplitude of the perturbation. To eliminate the imaginary damping term from (4.10), the necessary and sufficient condition for the marginal stability is

$$\frac{\mathrm{d}^2\Psi}{\mathrm{d}t^2}+(a_2^*+b_1^{*2}+q^*J_{\mathrm{f}}^2\cos^2\omega t)\Psi=0, \quad (4.17)$$

where a_2^*, b_1^* and q^* are the notations without a star given in (4.4), but under the restrictions given by (4.15).

For a uniform magnetic field $\omega\to 0$, the stability condition reduces to

$$J_{\mathrm{f}}^2>G \text{ or } J_{\mathrm{f}}^2<G, \quad (4.18)$$

depending on the sign of q^*,

where

$$G=-\frac{1}{q^*}(a_2^*+b_1^{*2}).$$

The examination for the increase of the rotation parameter Ω on the stability behavior is displayed in Figure 12. This figure shows the plane J_{f}^2 vs. R. J_{f}^2 is plotted for four values of the parameter Ω. The calculations showed that $q^*<0$, thus stability happens when $J_{\mathrm{f}}^2<G$. It is found that the parameter Ω has a stabilizing influence especially at large values of R.

As mentioned before, in the case of a periodic field, the stability criterion is given by

$$J_{\mathrm{f}}^2>G_1 \text{ and } J_{\mathrm{f}}^2<G_2;\ G_1>G_2, \quad (4.19)$$

where

$$G_{1,2}=\frac{8}{q^*}\Bigg[-(\omega^2-(a_2^*+b_1^{*2}))\pm(\omega^2-(a_2^*+b_1^{*2}))^{\frac{1}{2}}\left(\omega^2-\frac{3}{2}(a_2^*+b_1^{*2})\right)^{\frac{1}{2}}\Bigg].$$

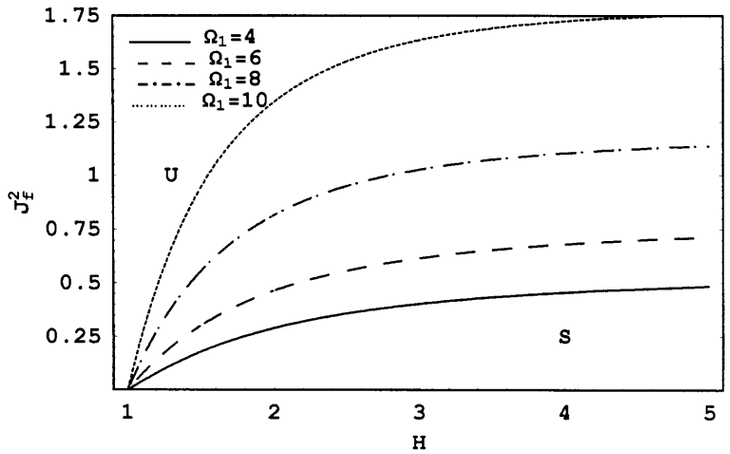

Fig. 10. Stability diagram for the same system as considered in Fig. 6, but when $\lambda = 1$, $\Omega_2 = 2$, $R = 2$, and for various values of Ω_1 The graph indicates the transition curves given by the inequality (4.13).

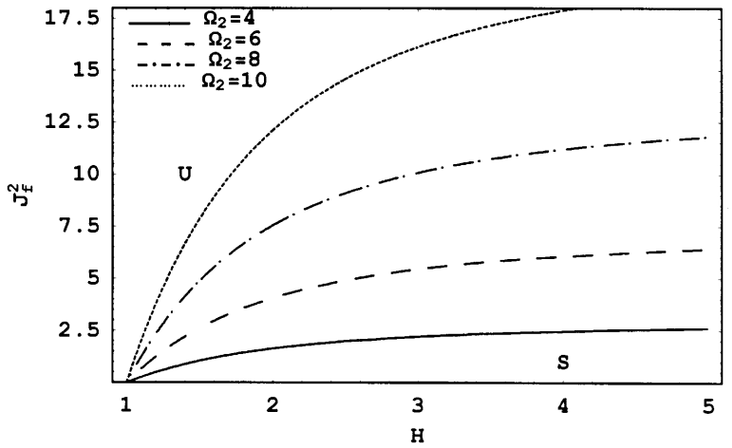

Fig. 11. Stability diagram for the same system as considered in Fig. 10, but when $\Omega_1 = 2$, and for various values of Ω_2 The graph indicates the transition curves given by the inequality (4.13).

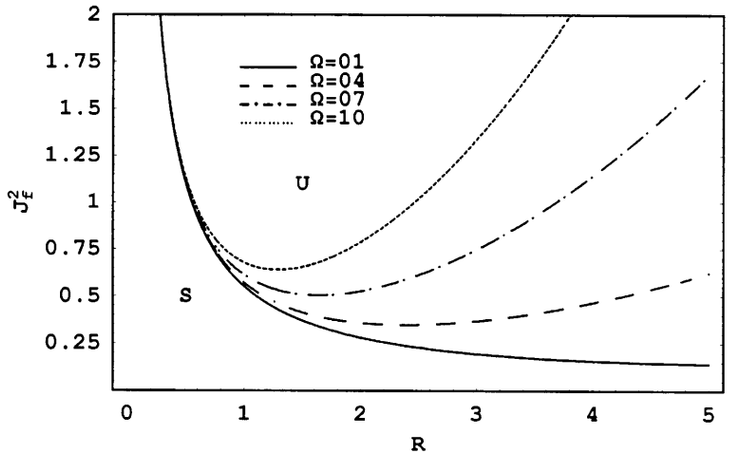

Fig. 12. Stability diagram for the same system as considered in Fig. 6, but when $\Omega_1 = \Omega_2 = \Omega$, and for various values of Ω. The graph indicates the transition curves given by the inequality (4.18).

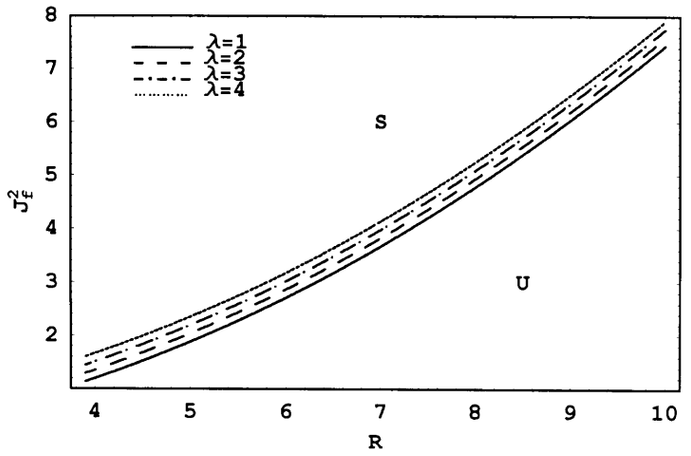

Fig. 13. Stability diagram for the same system as considered in Fig. 6, but when $\Omega_1 = 10$, $\Omega_2 = 5$, and for various values of λ. The graph indicates the transition curves given by the inequalties (4.22).

4.3. The Growth Rate Solution in Case B

In this section, we shall be concerned with the general case where the growth rate disturbance for the Mathieu equation (4.4) is presented. It is convenient to eliminate the imaginary damping term from (4.4) by making use of the transformation

$$\gamma(t) = \Re(t)\exp(-ib_1 t), \tag{4.20}$$

where $\Re(t)$ represents a time dependent amplitude of the perturbation. Equation (4.4) then becomes

$$\frac{\mathrm{d}^2\Re}{\mathrm{d}t^2} + 2a_1\frac{d\Re}{dt} + (b_1^2 + a_2 + qJ_\mathrm{f}^2\cos^2\omega t \tag{4.21}$$

$$+\ 2i(b_2 - a_1 b_1))\Re = 0.$$

In the case of a uniform magnetic field, the necessay and sufficient conditions for stability is given by

$$a_1 > 0 \text{ and } a_1^2(a_2+qJ_\mathrm{f}^2)+2a_1b_1b_2-b_2^2 > 0. \tag{4.22}$$

Thus the negative of the real part of the growth rate holds as the above conditions are satisfied. The transition curve separating the stable from the unstable regions is given by

$$J_\mathrm{f}^2 = \frac{1}{a_1^2 q}(b_2^2 - 2a_1b_1b_2 - a_1^2a_2). \tag{4.23}$$

The influence of the elasticity parameter λ on the stability behavior, in the case of a uniform field, is displayed in Figure 13. The calculations showed that $q > 0$. It follows that the surface currents play a stabilizing role. It is found that the increase of the parameter λ increases the unstable region. Therefore, the elasticity parameter λ has a destabilizing influence.

We now determine the stability conditions for the damped Mathieu equation (4.21). A perturbation technique may be used to accomplish this purpose. We use the method of multiple scales as described by Nayfeh and Mook [17] to obtain an approximate solution and analyze the stability criteria.

Since we are considering the surface deformations caused by the magnetic surface stress stemming from the alternating external magnetic field, for most cases studied in this work, it would be convenient to assume an ordering relation

$$J_\mathrm{f}^2 = \varepsilon J_\mathrm{f}^{*2}, \tag{4.24}$$

with J_f^* as a constant of proportionality.

In accordance with the method of multiple time scales, two time scales T_0 and T_1 are introduced such that

$$T_0 = t \text{ and } T_1 = \varepsilon t. \tag{4.25}$$

The details of this precedure are given in [14]. Omitting the details, one finds the stability criterion at the the resonance case of approaching the field frequency ω to the frequency part $\hat{\omega}$ of the growth disturbance in the form

$$\omega > \hat{\omega} + \frac{qJ_\mathrm{f}^2}{8(2\hat{\omega}^2 + a_1^2 - a_2 - b_1^2)} \cdot \left[2\hat{\omega} + \sqrt{3(a_2 + b_1^2) - 2\hat{\omega}^2 - 3a_1^2}\right], \tag{4.26}$$

$$\omega < \hat{\omega} + \frac{qJ_\mathrm{f}^2}{8(2\hat{\omega}^2 + a_1^2 - a_2 - b_1^2)} \cdot \left[2\hat{\omega} - \sqrt{3(a_2 + b_1^2) - 2\hat{\omega}^2 - 3a_1^2}\right], \tag{4.27}$$

provided that the stability conditions for the zero-order disturbance are satisfied. These conditions are

$$a_1 > 0 \text{ and } a_1^2 a_2 + 2a_1b_1b_2 - b_2^2 > 0. \tag{4.28}$$

In terms of the surface current density J_f, the stability conditions (4.26) and (4.27) are given by

$$J_\mathrm{f}^2 < \hat{J}_1 = \frac{8(\omega - \hat{\omega})(2\hat{\omega}^2 + a_1^2 - a_2 - b_1^2)}{q\left[2\hat{\omega} + \sqrt{3(a_2 + b_1^2) - 2\hat{\omega}^2 - 3a_1^2}\right]}, \tag{4.29}$$

$$J_\mathrm{f}^2 > \hat{J}_1 = \frac{8(\omega - \hat{\omega})(2\hat{\omega}^2 + a_1^2 - a_2 - b_1^2)}{q\left[2\hat{\omega} - \sqrt{3(a_2 + b_1^2) - 2\hat{\omega}^2 - 3a_1^2}\right]}, \tag{4.30}$$

where

$$\hat{w}^2 = \frac{1}{2}\left[\left\{(a_1^2 - a_2 - b_1^2)^2 + 4(b_2 - a_1b_1)^2 + a_2 + b_1^2 - a_1^2\right\}^{1/2}\right].$$

From the Floquet theory [17], the region bounded by

the two branches of the transition curves $\hat{J}_1$ and $\hat{J}_2$ is the unstable region. The region outside these curves is stable. The width of the unstable region is represented by $(\hat{J}_1 - \hat{J}_2)$. The increase of this width refers to the destablizing influence, while its decrease represents a stabilizing role.

[1] R. C. Sharma and V. K. Bhardwaj, Z. Naturforsch. **49a**, 927 (1994).
[2] P. Kumar, Z. Naturforsch. **51a**, 17 (1996).
[3] R. C. Sharma and P. Kumar, Z. Naturforsch, **52a**, 528 (1997).
[4] R. C. Sharma and P. Kumar, Z. Naturforsch. **52a**, 369 (1997).
[5] M. F. El-Sayed, Z. Naturforsch. **55a**, 460 (2000).
[6] Y. O. El-Dib, J. Plasma Phys. **65**, 1 (2001).
[7] S. Chandrasekhar, "Hydrodynamic and Hydromagnetic Stability", Oxford Univesity Press, Oxford 1961.
[8] Z. Alterman, Phys. Fluids **4**, 1177 (1961).
[9] P. G. Drazin and W. H. Reid, "Hydrodynamic Stability", Cambridge University Press, Cambridge 1981.
[10] C. H. Chung and W. Wuest, Acta Astronaut. **9**, 225 (1982).
[11] O. M. Phillips, J. Fluid Mech. **7**, 340 (1960).
[12] S. M. Sun, Phys. Fluids **6**, 1204 (1994).
[13] S. K. Wilson, Q. Jl. Mech. Appl. Math. **45**, 363 (1991).
[14] Y. O. El-Dib, J. Phys. A:Math. Gen. **30**, 3585 (1997).
[15] Y. O. El-Dib and G. M. Moatimid, Physica A **205**, 511 (1994).
[16] G. M. Moatimid and Y. O. El-Dib, Int. J. Engng. Sci. **32**, 1183 (1994).
[17] A. H. Nayfeh and D. T. Mook, "Nonlinear Oscillations", Wiley, New York 1979.
[18] Y. O. El-Dib, Chaos, Solitons and Fractals **12**, 705 (2001).
[19] G. M. Moatimid, Chaos, Solitons and Fractals **12**, 1239 (2001).
[20] Y. O. El-Dib and R. T. Matoog, J. Coll. Int. Sci. **229**, 29 (2000).
[21] J. R. Melcher, "Field Coupled Surface Waves", MIT Press, Cambridge, MA 1963.
[22] J. Q. Feng and K. V. Beard, J. Fluid Mech. **222**, 417 (1991).
[23] H. H. Woodson and J. R. Melcher, "Electomechanical Dynamics", Wiley, New York 1968.
[24] A. A. Mohamed and N. K. Nayyer, J. Phys. A: Gen. Phys. **3**, 296 (1970).
[25] R. Grimshaw, "Non-linear Ordinary Differential Equations", Blackwell Sci, Oxford 1990.